BULLETIN OF THE POLISH ACADEMY OF SCIENCES
TECHNICAL SCIENCES
DOI: 10.24425/bpasts.2026.157322

The study on the effect of blade guide strip on aerodynamic performance of horizontal axis wind turbine

Guowen LI[1] Haotian SONG[1] Xinghui WU[1] Xinhua SUN[1]

[1] Shenyang Aerospace University, Shenyang110136, China

Abstract: This paper mainly studies the influence of adhering hidden movable airflow guide strips to the surface of horizontal-axis wind turbine blades on the aerodynamic performance of the blades. The experimental data suggest that the guide strip changes the flow direction of the airflow. A reverse force will be generated in the opposite direction of the airflow outflow, i.e., the blade guide strip's resistance and the airflow's flow distance on the blade surface will be increased. The lift of the blade will be increased with a low starting wind speed and a significant wind energy utilization effect. The research results show that the guide strip structure can increase the lift coefficient of the blade by 9.1% under the condition of a small Angle of attack. When the wind speed reaches 8 m/s, the power coefficient increases by 14.1% and the starting wind speed decreases by 0.5 m/s. However, the negative resistance of the guide strip was increased at high incoming flow speeds. At this time, the guide strip was adopted to level the actuator and placed on the blade's surface. The experimental results show that when the guide strip is retracted, the output power of the wind turbine is the same as that of the prototype blade.Therefore, the guide strip blades with retraction and extension functions enhance the low-speed performance of the wind turbine while maintaining its high-speed performance.

Key words: Guide strip; Wind turbine; Wind tunnel test; Lift-drag conversion;

1. INTRODUCTION

Increasing wind turbines' wind energy utilization rate is a vital direction and takes on great significance in the research of wind energy power generation. However, increasing the wind energy utilization coefficient requires improving the wind turbine's overall performance. Wind turbine blades absorbing wind energy have become a critical research topic. In general, the extensively used horizontal axis wind turbines belong to the lift type, which depend on the blade lift's tangential force in the rotating profile to provide power. Horizontal-axis wind turbines have been demonstrated as the most effective conversion device in practice, currently accounting for over 99% of all wind power generation installations[1]. However, horizontal-axis wind turbines also exhibit fatal weaknesses. The horizontal-axis wind turbines have a relatively large starting torque, and the starting wind speed should be slightly higher. Thus, the working wind speed requirements are relatively high, while the working area and time are relatively strict. Accordingly, how to reduce the starting wind speed of horizontal-axis wind turbines and enhance their low-speed performance is regarded as the technical difficulty of the existing research on horizontal-axis fans, so extensive studies have been conducted to enhance the performance of the blades. For instance, there are articles on blade flow control, including green flap, rough belt, pitch, blade head jet, plasma, and other works of literature [2,3,6,8-14]. There are also articles on blade structure vortex generators and suction surface wave stripes, including blade tip sweep, blade thickness, blade shape, etc. [5,7,15,16].

In the flow control of blades, Gurney flaps first appeared in the probability of Gurney flaps improving airfoil aerodynamic performance proposed by Liebeck[17] in 1978. Subsequently, Aryan Tyagi et al[18]. proposed a new framework for optimizing the Gny flap using the radial basis function neural network and the bugu search algorithm. By training on the CFD data of the two-dimensional Reynolds average Navier-Stokes simulation, the optimal design parameters of the Gny flap were obtained. The optimized Genny flap configuration has increased the lift-to-drag ratio by 10.28%. Keren Lin et al[19]. adopted the direct simulation Monte Carlo method to study the aerodynamic optimization problem of the NACA 0012 airfoil with Gny flaps attached in raretenent gas flow. Through multi-objective aerodynamic optimization and the construction of an artificial neural network model, the lift-to-drag ratio of the airfoil was increased by up to 29.25% under different Mach numbers and

*e-mail: songhaotian1@stu.sau.edu.cn

Knutsen numbers. In the fields of eddy vortex generators, adaptive flaps, seam wings and trailing edge deformation, Jia et al[20]. adopted the wind tunnel test method to systematically study the Reynolds number effect of the vortex generator on the aerodynamic performance optimization of wind turbine airfoals within a continuous large Reynolds number range. The results show that with the increase of the Reynolds number, the airfoil lift coefficient presents a significant growth trend, and the different placement positions of the vortex generator have different effects on the improvement of the airfoil lift coefficient. Li et al[21]. designed a superhydrophobic convex windmill. Its blades integrate a flexible trailing edge structure with active deformation. The trailing edge is adaptively adjusted through the humidity response characteristics of the material, and the fog collection and power generation functions are simultaneously realized, providing a model for the research and development of multi-functional integrated flow control equipment. Qin et al[22]. studied the combined regulation ability of S-shaped grooves and trailing flaps on the aerodynamic characteristics of wind turbine blades. The results showed that this combined control strategy could significantly improve the stall phenomenon of the airfoil at high angles of attack, thereby significantly enhancing the ability of the trailing flaps to control the lift coefficient. Taurista P. Sya Witri et al[23]. studied the improvement of the aerodynamic performance of lift-type vertical-axis wind turbine blades with slit-improved Gni flaps. The results showed that at a medium sharp-speed ratio, the blade drag of the slit-improved Gni flaps was significantly reduced by 8%, although the lift was reduced by 2% compared with the clean Gni flap blades. However, it has increased the lift-to-drag ratio and enhanced the generation of torque. Abolfazl Abdolahifar et al[24]. conducted a comprehensive three-dimensional study on the Dalihe vertical-axis wind turbine with slit blades, aiming to reduce flow separation. Through numerical simulation, the aerodynamic performance of different slit blade designs and their corresponding flow field structures were precisely analyzed. Regarding parameter optimization, Tanurun[25] optimized the aerodynamic performance parameters of vertical-axis wind turbines. By using the Taguchi method to optimize three parameters, and combining ANOVA and regression analysis to clarify the contribution of parameters and construct a high-fitting prediction equation, it filled the research gap in multi-parameter collaborative optimization and high-precision prediction. Regarding wind tunnel tests, Strojny[26] conducted wind tunnel and field tests for small horizontal-axis wind turbines, proposed a new rotor concept suitable for low-speed wind and capable of enhancing efficiency, introduced the calculation methods of rotors and generators, briefly described the structural scheme of the unit, component manufacturing and assembly processes, and analyzed the test results to verify the improvement effect of the new rotor on the utilization efficiency of low-speed wind energy. There are also studies on the flow control structure of biomimetic blades. Researchers have found that the characteristics of some animals such as humpback whales have greatly improved their movement speed and predation flexibility, so they have carried out research on biomimetic blade structure[27]. Syed Saddam ul Hassan et al[28]. systematically studied the relative influence of bionic leading edge nodules on the power boost of vertical-axis wind turbines. By using the mixed experimental design method and the response surface method, they resolved the contradiction in the literature regarding the influence of nodules on the power performance of vertical-axis wind turbines. HR Kaviani et al[29]. conducted numerical simulation studies on the impact of adopting bionic airfoals (the cross-section of seagull wings) in horizonte-axis wind turbines on performance. The results showed that the power generation of the turbines increased significantly at different wind speeds. Chetan S. Nalavade et al[30]. studied the Savonus wind turbine rotor blades inspired by the sea pen. The results showed that within a given wind speed range, the performance of the sea pen blades was improved by approximately 10%-13% compared to the semi-circular blades. Compared with the many control techniques mentioned above to improve the aerodynamic performance of blades, the guide strip structure studied in this paper is a brand-new passive control technology.

Wind turbines use wind energy in the following forms: 1) The lift type has been widely used since it can have a higher wind energy utilization coefficient, and it is the most common application method for the horizontal axis. 2) Resistance type, with a relatively small TSR, is easy to start, but its wind energy utilization rate is not high. 3) Lift-and-drag hybrid type. This combination combines the above two disadvantages, whichever is advantageous, whereas the resistance unit will become the resistance of the entire fan at a large tip speed ratio.

If the resistance unit is combined with the lift blade structure, it can reduce the negative effect caused by the resistance unit while improving the deficiency of the lift blade. Thus, this lift-type mixed resistance blade has promising applications and development. A novel form of wind energy utilization was proposed in this study following the idea of a lift-drag hybrid blade, namely a lift-drag conversion blade. The guide strip was installed on the horizontal axis lift blade. When the impeller rotated at low speeds, the guide strip can act as a resistance element and decrease the starting wind speed of the fan. When the impeller rotated at high speeds, and the guide strip hindered the rotation of the impeller, the actuator in the blade was adopted to hide the guide strip so as not to change the high-speed performance of the fan blade, and the blade was converted into the lift type. The flow guide strip is controlled by microcircuits. It is a thin sheet with a slight flexibility. By using a micro-motion motor push rod, it can drive the connecting rod installed on the flow guide strip, causing the flow guide strip to move from 0 degrees to 90 degrees. The guide strip can be attached to the surface of the blade and perpendicular to it. Realize the control of the flow at the boundary of the blade surface by the guide strip. The pull rod can be arbitrarily controlled by the control unit, and the guide strip is raised and lowered through the motion of the linear motor in the control unit, as presented in Fig. 1. At present, the flow control technology of guide strip to blade is

an extension and supplement to the previous flow control technology, and there is no similar flow control technology.

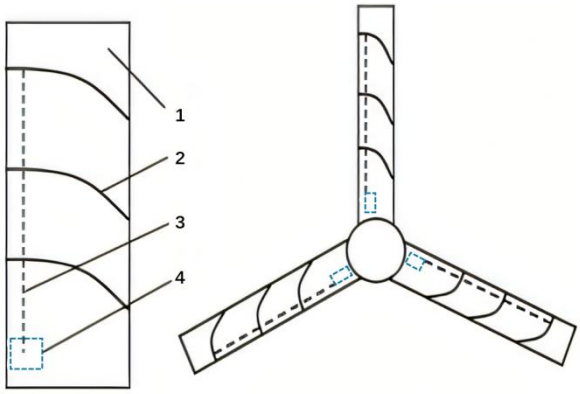

1 blade 2 guide strip 3 pull rod 4 control unit

Fig.1. Guide blades and wind wheels

2. EXPERIMENTAL DEVICE AND METHOD

The wind tunnel employed in the experiment of this study was the SHDF low-speed closed-loop return wind tunnel of Aeroengine College of Shenyang Aerospace University. The test section was 3.5 m in length and 1 m × 1.2 m in cross-section, with a maximum adjustable wind speed of 50 m / s.

Table 1. Wind tunnel flow field parameters

Maximum speed（m/s）	50
Minimum stable speed（m/s）	5
axial static pressure gradient|dCp/dx|(l/m)	≤0.005
Field coefficientμi	0.0045
Mean airflow angle|α|	≤0.5°
Mean airflow angle|β|	≤0.5°
temporal stabilityη	0.005
turbulence	≤0.14%

2.1. Research methods and experimental models

In this study, the experimental study on the effect of guide strip height on blade performance was first carried out. The research data was obtained from blade pressure measurement experiment. The effect of guide strip on the aerodynamic performance of the blade was determined through the experimental results, so as to evaluate the advantages and disadvantages of the flow control method. Subsequently, the effect of the different offsets of the front and rear edges of the guide strip on the aerodynamic performance of the horizontal axis wind turbine was obtained following the experimental results to select the optimal height and offset. Lastly, the guide bar was installed on the blade with the actuator to study the overall performance of the wind turbine through experiments.

The blade pressure test model adopted the metal model with a chord length of 300 mm and the type of 0417 airfoils, the pressure measurement cross-section is in the center section of the blade, i.e. 50% of the extended blade spread. The guide strips were arranged to extend the blade span to 25 %, 50 %, and 75 %, respectively, with a thickness of 1mm, and the material was soft plastic. With the blade frontal line, the angle was 90°, and with the blade posterior frontal line, it was 45°. Taking the deflection of the flow guide strip at 0.5% thickness, 1% chord length and 33.3% deflection as an example, a schematic diagram of the flow guide strip size was made, as shown in Fig. 2. The horizontal axis experimental fan adopted three wooden blades with uniform circumferential arrangement. Fig. 3 presents the experimental device. The wind wheel of the experimental fan model had a diameter of 0.6 m, the height of the centerline was 0.5 m, and the blades were rectangular and straight blades without twisting. The blade type was NACA0018 airfoil. The chord length of the blades was the same along their height, which was 60 mm. The guide strips were arranged to extend 25%, 50%, and 75% of the blade extension, respectively, with a thickness of 0.3 mm, and a substance of soft plastic. The angle between the forehead lines of the blade was 90°, and the angle between the forehead lines of the blade was 45°. The blade guide strip retracting device was created utilizing the single-chip microcomputer to collect the speed signal and automatically control the electromagnetic action pull rod. The setting parameters were obtained in the experiment.

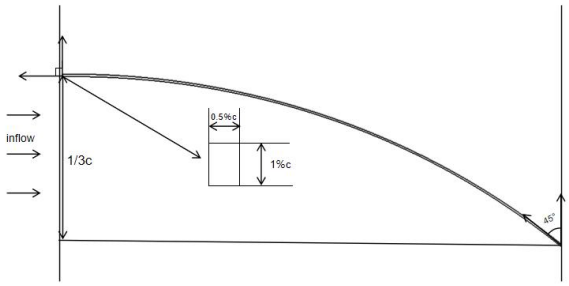

Fig.2. Schematic diagram of the flow guide strip size

2.2. Measure equipment

The DSY-JB of Northwestern Polytechnical University was adopted in the pressure scanning valve of the pressure test, which is a pressure test system integrating pressure measurement, data acquisition, online calibration, and data processing. The main feature of this system is to achieve multi-point, fast, and high-precision pressure measurements. The pressure scanning valve system can increase the efficiency of pressure measurement while also improving the quality of experimental data and the reliability of the experiment. The pressure measurement channel had 96 points, with an accuracy of ±0.2% FS, the scanning rate was 20000 points/sec, and the range was ±2.5 KPA (64 channels) ±7.0 KPA (32 channels).

The torque and speed of the experimental fan were measured by the AKC-215 dynamic torque and speed sensor of Beijing 701 Institute, and the torque and speed signals were output simultaneously. The load regulation system comprised a CA-0.2 magnetic powder brake and WLK-1A controller.

Fig.3. Wind turbine experimental device

Fig.4. Experimental model of blade guide bar pressure measurement

3. THEORETICAL BASIS FOR GUIDE STRIP DESIGN

The leaf element theory analyzes the stress and functional exchange on the blade from the flow close to the leaf element. The leaf is divided into several segments along the spreading direction, each referred to as a leaf element. It is assumed that there is no interference between each micro-segment, and the force acting on the respective leaf element is solely determined by the lift-drag characteristics of the leaf element's airfoil. The leaf element can be considered a binary airfoil. On that basis, the force and moment acting on each leaf element along the spanwise direction, and the force and moment acting on the wind wheel can be calculated.

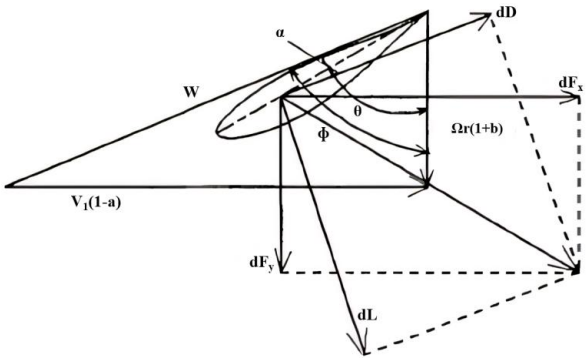

Fig.5. Force and velocity triangle of leaf profile

The last circumferential thrust and moment of the ring element at the wind wheel radius r are written as follows:

$$dL = \frac{1}{2}\rho W^2 C C_L dr \quad (1)$$

$$dD = \frac{1}{2}\rho W^2 C C_D dr \quad (2)$$

$$dF_x = dL\cos\phi + dD\sin\phi = \frac{1}{2}\rho W^2 C dr C_x \quad (3)$$

$$dF_y = dL\sin\phi - dD\cos\phi = \frac{1}{2}\rho W^2 C dr C_y \quad (4)$$

$$dT = BdF_x = \frac{1}{2}\rho W^2 BC dr C_x \quad (5)$$

$$dM = BdF_y r = \frac{1}{2}\rho W^2 BCC_y r dr \quad (6)$$

Where (Fig. 5) B denotes the number of blades; ρ represents air density; W is combined speed; C expresses blade chord; C_x is the axial force coefficient of wind shaft; C_y is the normal force coefficient of wind shaft; α is the axial inducer; b represents the circumferential Inducer; ϕ is the Inflow angle of blade; θ is the blade incidence; α is the Leaf element angle of attack; V_1 is the velocity of wind flow; Ω denotes the rotor speed; r is the distance from blade profile to wind wheel center.

Accordingly, without modifying the original blade parameters, the force on the blades can only be changed by adjusting the incoming wind speed, i.e., allowing the horizontal axis fan to get a large thrust at high speed. The velocity triangle in Fig. 5 indicates that when the blades are stationary, the incoming flow velocity is the combined velocity, and the blade installation angle is the actual angle of attack. As a result, all that is needed is to increase the rotational tangential force of the blade. Subsequently, the starting wind speed of the fan can be lowered. If the guide strip is installed on the blade, it obstructs the flow of airflow, and part of the airflow on the blade's surface will flow out at a 45° angle to the blade in the direction of the guide strip. The momentum theorem suggests that it will be produced in the opposite direction of the speed. Acting force, or the component of the force in the direction of the blade rotation, is the thrust, and since the airflow is accelerated under the action of the guide strip, the blade's lift will also increase. Blade performance can be improved when operating at constant speed. When the impeller is started, the impeller's combined speed and the air attack angle are increased with the increase of the impeller speed. The guide strip cannot guide the airflow to turn, so its function is lost, and it acts as a resistance element, whereas it hinders the rotation of the impeller. As a result, the guide strip is put down, the blades return to the original aerodynamic shape, and the resistance type is converted to the lift type, resulting in the maintained aerodynamic performance of the original blades.

4. EXPERIMENT AND RESULT ANALYSIS

A pressure test was performed on the blade first, followed by a pressure distribution experiment on the blade surface at various guide strip heights to investigate the effect of installing a guide strip device on the surface of a wind turbine blade on wind turbine performance. The results were compared and analyzed. Subsequently, the wind turbine computer simulation experiments were conducted on the blades at various guide strip heights using the results of the pressure measurement data to determine the guide strip parameters. Next, the wind tunnel experiment on the lift-drag conversion of the blade installation guide strip was carried out, followed by a series of wind tunnel comparison studies under various operating situations.

4.1. Blade pressure distribution experiment

The blade pressure distribution experiment selected the guide strips with 0.5%, 1%, and 2% blade chord height, respectively. The selection of the height of the guide strip is determined by the thickness of the boundary layer, and the height of the guide strip is obtained by equal division according to the boundary layer scale. The offset of the front and rear edges of the guide strip was 33.3% of the chord length, and only the guide strip was pasted on the suction surface of the blade. The measurement accuracy of the pressure scanning valve was selected at the optimal point to ensure the accuracy of the pressure measurement experiment, and the wind speed of the experiment was equivalent to 30 m/s. The angles of attack measured in the experiment are -4°, 0°, 4°, 6°, 8°, 12°, 14° and 16°. The selection of these angles of attack is based on the common Angle of attack of wind turbine blades.

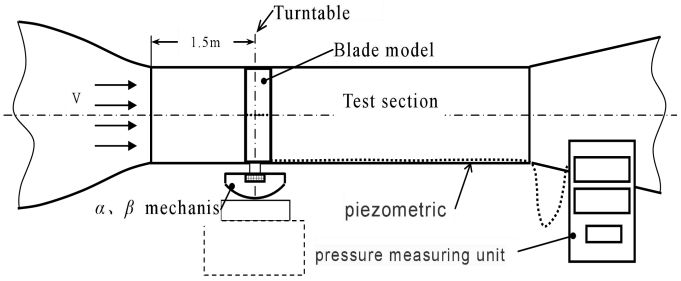

Fig.6. Installation diagram of blade pressure test model

The experimental blade is based on the all-aluminum model NPU-0417. The wingspan is 996 mm, the chord length is 300 mm, the maximum thickness of the airfoil is 51 mm, the wing area is 0.3 m2, and the rotation center is located at 25% of the chord length, as shown in Fig. 7.

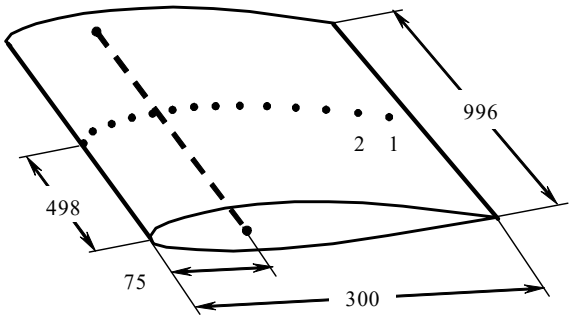

Fig.7. Binary airfoil diagram

The blade pressure measurement model had 15 pressure measurement holes on the upper and lower airfoil surfaces of the middle section, and there was a pressure measurement hole on the leading edge. The measured surface pressure was converted into a pressure coefficient:

$$C_p = \frac{p_i - p_\infty}{\frac{1}{2}\rho V_\infty^2} \tag{7}$$

Where P_i denotes the measuring surface static pressure; p_∞ is the far forward static pressure, take the static pressure measured by the Pitot tube at the entrance of the test section; V_∞ represents the incoming flow speed; ρ is the air density.

The blade pressure distribution curve was generated with the ratio of the distance x from the measuring point to the leading edge of the blade to the chord length b as the abscissa and with the pressure coefficient of the measuring point as the ordinate.

Measurement error: The data acquisition signals of the wind turbine experimental device mainly include: experimental wind speed, wind turbine impeller speed, wind turbine output torque, wind turbine output shaft power, etc. The wind turbine signal outputs±15 KHz signal through the torque meter, which is converted into an analog quantity after being converted by the signal conditioning module, and the data is collected by the acquisition card. The signal acquisition process is under stable wind speed. When the wind turbine speed is stable, the input current of the magnetic powder brake is adjusted to increase the wind turbine load, and data is collected when the output is maximum. In order to ensure the reliability of the data, the data of the same working conditions were collected for one minute, and the average value was obtained. The accuracy of each equipment in the system is as follows: the accuracy of torque meter is 0.2% FS, the accuracy of wind speed control is 0.45%, the accuracy of signal conversion module is 0.1%, the accuracy of signal acquisition card is 16 bits, that is, 1/216. Therefore, the total accuracy of the experimental test is:

$$e_{RSS} = \sqrt{e_N^2 + e_V^2 + e_M + e_{AD}^2} = \sqrt{0.002^2 + 0.0045^2 + 0.001^2 + \left(1/2^{16}\right)^2} \approx 0.5\%$$

The total test accuracy of the system is 0.5%, which meets the testing requirements of wind turbine performance experiment, and the test data is highly reliable.

Fig. 8 compares the blade pressure distribution curves for various guide strip heights. As seen in the figure, the height of

the guide strip had an impact on the distribution of the blade surface pressure. When the chord height of the guide strip was 1%, the pressure coefficient of the blade's leading edge was decreased significantly. Thus, this study focused on the effect of the 1% height guide strip on the pressure distribution of the blade. Fig. 9- Fig. 10 indicate that with the increase of the angle of attack of the blade, the pressure coefficient of the suction surface of the blade decreased first and then increased and reached the optimal value when the angle of attack was 6°. The blade wall pressure was consistent with the mainstream pressure on the blade normal due to the presence of a boundary layer on the blade surface. However, in this study, the guide strip primarily controlled the flow in the boundary layer. As depicted in Fig. 8, when the height of the guide strip was too low, the guide strip was completely submerged in the viscous bottom layer, thus having a slight effect on the mainstream. When the guide strip was too high, it entered the main flow area, the effect of the guide strip on the main flow was extremely large, and the main flow energy was reduced. Only when the height of the guide strip is in the transition zone can it effectively control the flow in the boundary layer and marginally affect the mainstream. Moreover, the change in pressure coefficient with the blade angle of attack helps explain the aforementioned issue. The greater the angle of attack, the greater the thickness of the boundary layer will be. Furthermore, the guide strip tends to be submerged in the viscous bottom layer, and its guiding impact on the mainstream is lost, and the pressure distribution of the blade remains unaffected. When the blade angle of attack increases, the airflow on the upper surface of the blade separates, and the high guide strip can increase the main flow and airflow doping within the boundary layer, suppressing the separation of the airflow and achieving the blade's performance of increasing the stall angle of attack, as shown in Fig. 11.

Accordingly, the guide strip can help increase lift at a small angle of attack while inhibiting airflow separation at a large angle of attack.

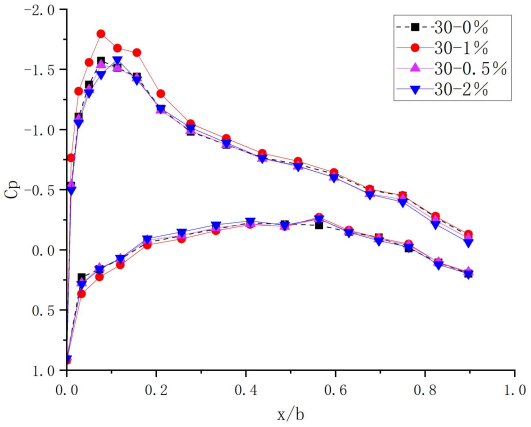

Fig.8. Comparison curve of pressure distribution of different height guide strip for blades with 4°angle of attack

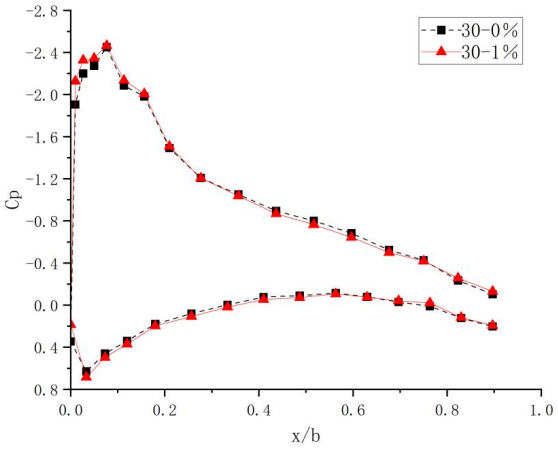

Fig.9. Comparison curve of pressure distribution of blades 6° angle of attack and 1% height guide strip

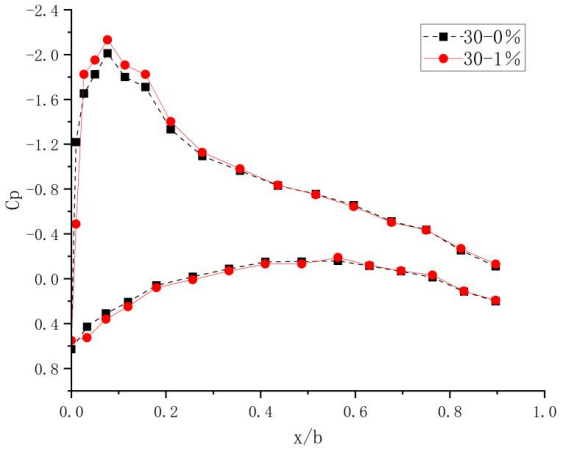

Fig.10. Comparison curve of pressure distribution of blades 8°angle of attack and 1% height guide strip

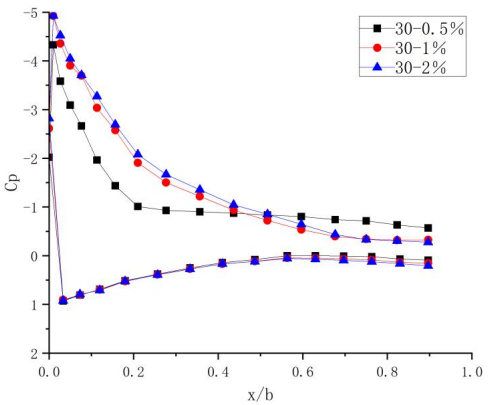

Fig.11. Comparison curve of pressure distribution of different height guide strip for blades with 16°angle of attack

4.2. Simulation calculation analysis of blade guide strip

In this study, the associated region of computation and boundary conditions are shown in Fig. 12. The meshing is done by using Fluent Meshing to generate a high-quality unstructured hybrid mesh with localized encryption around the airfoil and its nearby critical regions.

This article uses ANSYS Fluent software to run numeri cal simulations with a k-ω SST model. The output is configu red as a pressure outlet with a gauge pressure of 0, and the in take i s configured as a velocity inlet with a velocity of 30 m/ s. The SIMPLEC technique is used to obtain the pressure-vel ocity coupling term. All physical quantities' relaxation factor s are set to the Fluent software's default values. Green-Gauss Node-based interpolation is used to achieve the gradient high dispersion, and the pressure term follows a standard format.

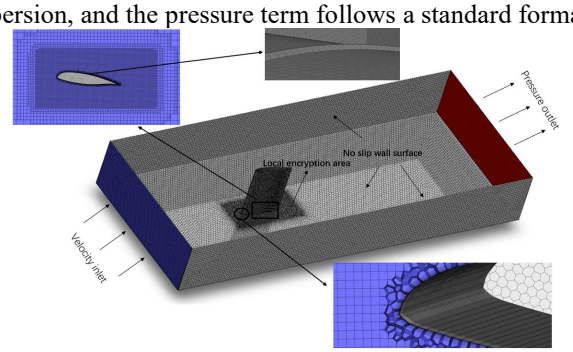

Fig.12. Schematic diagram and boundary conditions of computational domain grid

In order to verify the accuracy of the simulation results, the irrelevance analysis was carried out on the base blades with three different mesh densities, and the angles of attack were selected as 6°, 12° and 16°, respectively, to analyze the influence of different mesh numbers on the simulation results of airfoil lift coefficient, as shown in Fig. 13. It can be seen that when the number of grids reaches 3.5 million, the lift coefficient of the blade basically remains stable. Considering the calculation cost and efficiency comprehensively, 3.5 million grids were selected for numerical simulation analysis and the grid y+ on the airfoil surface is less than 1, meeting the calculation requirements.

Fig. 14 shows the pressure coefficient distribution of the base blade when the Angle of attack α =6°. The results show that all the turbulence models used can produce results similar to the experimental results.

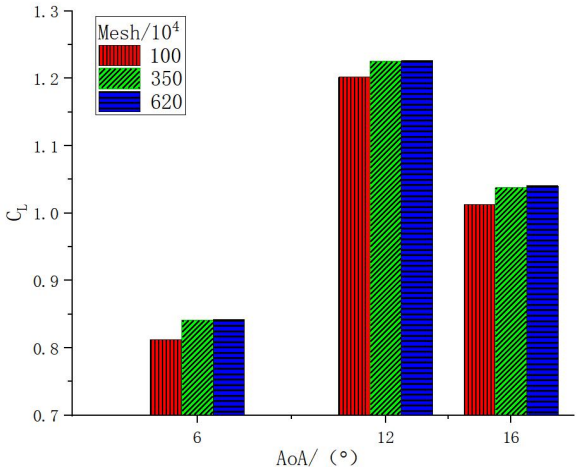

Fig.13. Mesh independence analysis of lift coefficient for base blade

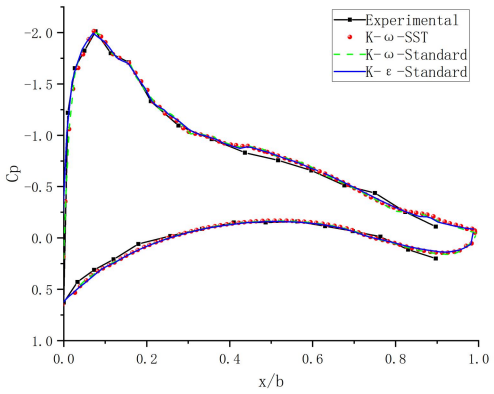

Fig.14. Pressure coefficient distribution curves of base blades under different turbulence models when the Angle of attack of incoming flow is 6°

In order to verify the correctness of the model, the lift coefficient of NPU-0417 blade at an incoming flow velocity of 30m/s was calculated, and the calculated results were compared with the experimental results, as shown in Fig. 15. It can be seen from the figure that the numerical calculation of lift coefficient is basically consistent with the experiment, which proves that the numerical calculation method in this paper is reliable.

Fig. 16 shows the comparison between the numerical calculated lift coefficient of the base blade and the guide strip blade at the Angle of attack from 0° to 8° and the experimental lift coefficient. It can be seen that there is little difference between the numerical calculated results and the experimental results, and it is once again proved that the guide strip can improve the lift coefficient of the blade with an Angle of attack below 8°.

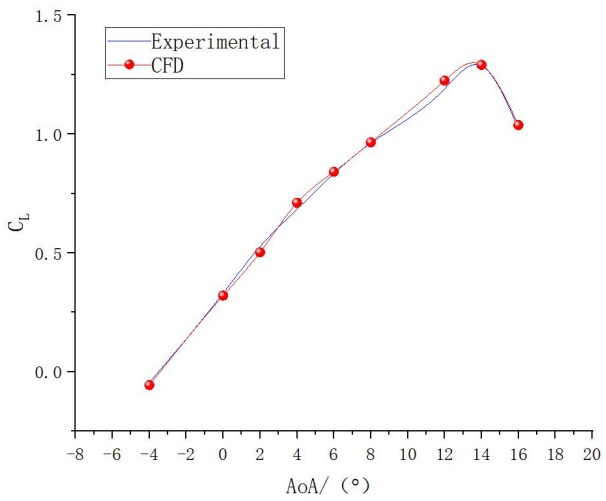

Fig.15. Validation of calculation model

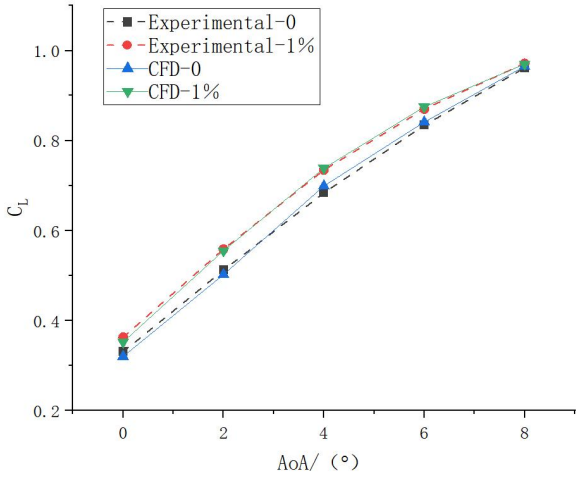

Fig.16. Numerical and experimental comparison of lift coefficients of base blade and guide strip blade

As illustrated in Fig. 17, 18, and 19, eddy currents are generated near the trailing edge of the blade's upper surface due to the influence of the flow guide strip. This vortex induces airflow on the upper surface of the blade and decreases its pressure coefficient, thus, the lift coefficient of the blade is increased.

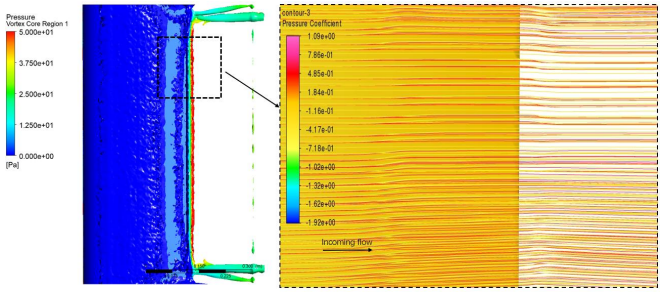

Fig.17.6°Angle of attack blade without guide strip, eddy current diagram of upper surface and flow diagram near trailing edge

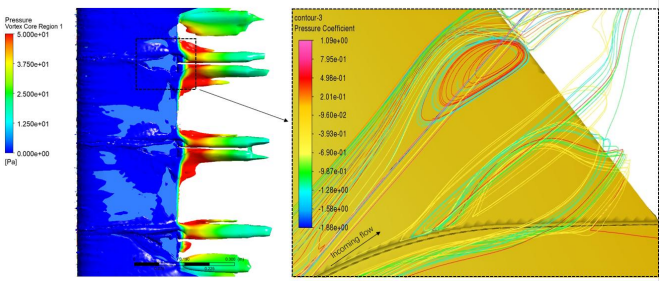

Fig.18.6°Angle of attack 1% chord length guide strip blade, upper surface vortex diagram, near trailing edge flow

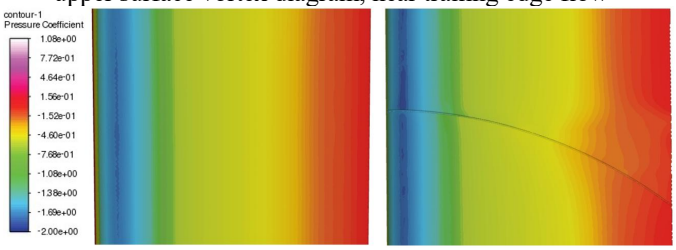

Fig.19. Cloud image of pressure coefficient near the guide strip on the upper surface of the 6° Angle of attack blade

4.3. Guide strip parameter calculation

The parameters of the guide strip were obtained through computer simulation. The height and offset of the guide strip were primarily studied, and a three-dimensional model of the impeller with a chord length of 300 mm was built. The parameters in the table were given as a dimensionless percentage of the blade chord length. Nine working conditions were calculated. The impeller's low-speed performance was investigated. The given wind speed was 6 m/s while the rotational speed was 1000 r/min. Table 2 lists the working conditions of the calculation model. The results in Table 3 showed that when the guide strip hindered the rotation of the impeller with the guide strip of 6%, it had a slight effect on the torque of the impeller with the guide strip of 0.5%, the increase in torque was the largest at 1%, and the comprehensive performance of the guide strip and the blade was optimal when the offset was 33%. Lastly, the parameters were obtained for the wind tunnel experiment of the wind turbine.

Table 2. Guide strip parameter calculation conditions

Installation angle	Thickness	Height	Offset
6°	0.5%	0.5%	25% , 33%, 50%
6°	0.5%	1%	25% , 33%, 50%
6°	0.5%	2%	25% , 33%, 50%

Table 3. Calculation results

Height	Offset	Wind speed （m/s）	Rotating speed (r/min)	Torque (NM)
0.5%	25%	6	1000	0.098
	33%			0.113
	50%			0.010
1%	25%			0.184
	33%			0.225
	50%			0.193
2%	25%			0.004

33%	-0.012
50%	-0.055

4.4. Wind turbine starting torque experiment

When the test unit was unloaded, and the wind wheel was in a free state, the wind tunnel was activated, and the wind speed was stabilized. The torque on the wind wheel shaft was measured at the starting wind speed of the wind wheel. This test collected data for one minute at an 8 m/s wind speed, and the average value was calculated.

Table 4. Comparison of starting wind speed and torque

starting torque		Starting wind speed	
Guide strip blade	No guide strip blades	Guide strip blade	No guide strip blades
0.445 N·m	0.368 N·m	6.2m/s	6.7m/s

4.5. Experiments on aerodynamic characteristics of wind turbines

The guide strip installed on the blade can change its attitude under the control of the single-chip microcomputer, and the control parameters should be obtained during the test. Thus, the wind turbine performance test was divided into three parts, including 1. Guiding strip hiding test; 2. Guiding strip opening test; 3. Guiding strip opening and hiding conversion joint experiment. Through 1 and 2 experimental studies, the hidden speed nodes of the guide strip were obtained, and the aerodynamic performance of the fan's two working conditions was compared through the experimental data analysis. Lastly, the 3 experimental studies verified that the guide strip enhances the wind turbine's low-speed performance without affecting its high-speed performance.

The power output curve of the wind turbine, when the guide strip was opened, is shown in Fig.20. In the figure, close indicates that the guide strip is hidden, and open indicates that the guide strip is released. At low wind speeds, the effect was significant once the blade was equipped with a guide strip, as shown in this figure. As wind speed increased, the increasing trend of output power tended to decrease. When the wind speed exceeded 12 m/s, the function of the guide strip was completely invalid, consistent with the blade design.

Combine Fig. 21 and Table 5, when the wind speed was 8 m/s, the resistance of the guide strip was significant, and the power coefficient has increased by 14.1%. The power coefficient had an inflection point as the wind speed increased. In contrast, the prototype blade's inflection point was insignificant, and the downward trend was gentle. Thus, the function of the guide strip to guide the airflow tended to be replaced by the impeller rotation speed due to the faster increase of the impeller joining speed of the guide strip blades. The direction of the airflow in the boundary layer of the blade changed, and the spanwise flow of the airflow was limited to a certain range due to the existence of the guide strip, thus increasing the flow resistance and reducing the airflow energy. Furthermore, the impeller's absorption work inevitably decreased. Fig. 20 and Fig. 21 also prove this argument.

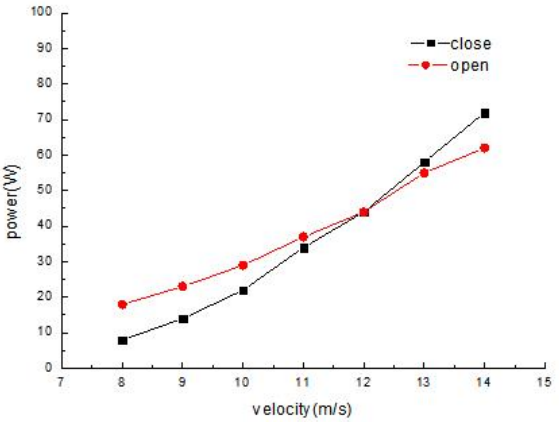

Fig.20. Fan output power characteristic curve

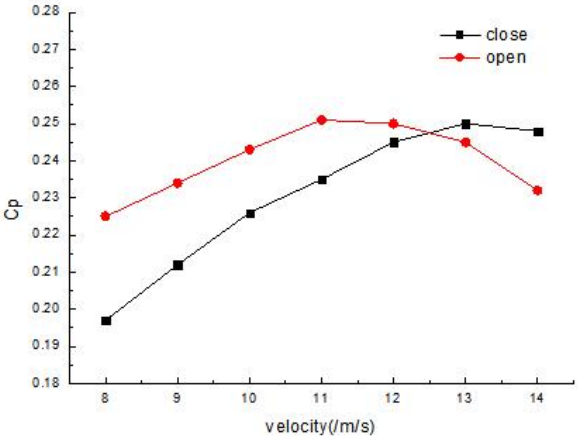

Fig.21. Wind energy utilization coefficient curve of wind turbine

Table 5. Percentage increase in power coefficient

Velocity（m/s）	8	9	10	11	12
Percentage increase in cp（%）	14.1	10.3	7.1	6.9	2.2

4.6. Performance experiment of wind turbine controlled by guide strip retraction

To solve the shortcomings of low-speed lift-type horizontal-axis wind turbines that are difficult to start, blade guides were adopted to enhance the low-speed performance of lift-type horizontal-axis wind turbines and reduce the wind turbine's starting wind speed, which is equivalent to adding drag elements on the blades. However, as indicated in Fig. 20 and 21, the guide strip hinders the high-speed rotation of the blade. Accordingly, this study investigated a blade that can retract the guide strip to successfully realize the conversion of the blade from the drag type to the lift type. The guide strip was retracted and controlled through an electromagnetic push rod and manual remote control.

According to the graph in Fig. 20, when the wind speed was 12 m/s, the function of the guide strip was rendered ineffective, and the corresponding wind wheel speed was 1500 rpm. Thus, the manual control guide strip retracted the speed

node to 1500 rpm, the power output curve of the wind turbine under combined control of the guide strip was obtained and shown in Fig. 22. In the figure, open-close union indicates the combination of the hidden guide strip and the released guide strip. The figure illustrates that when the guide strip was retracted, the wind turbine's output power remained the same as the prototype blade, and the blade's lift performance was unaffected after the guide strip was hidden. Accordingly, the guide strip blade with retractable function enhances the low-speed performance of the wind turbine while maintaining the high-speed performance.

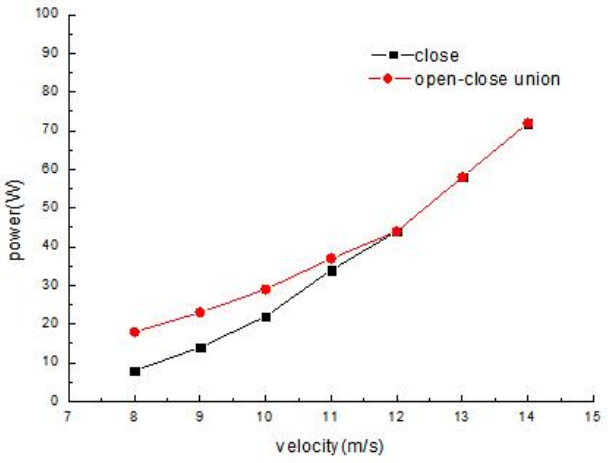

Fig.22. Aerodynamic characteristic curve of the fan

5. CONCLUSION AND DISCUSSION

The analysis of experimental data and simulations demonstrates that guide strip blades boost blade lift and improve the wind turbine's low-speed performance. The research results show that the guide strip structure can increase the lift coefficient of the blade by 9.1% under the condition of a small Angle of attack. When the wind speed reaches 8 m/s, the power coefficient increases by 14.1% and the starting wind speed decreases by 0.5 m/s. The wind turbine produces a high output even at low wind speeds. It is appropriate for the low wind speed operating environment of the horizontal axis wind turbine, broadens the wind speed range of the wind turbine, and removes reliance on the wind field. This technology is more consistent with the existing circumstances and the development needs of domestic wind energy use. In addition, the guide strip blade with retractable function studied in this study is a form of lift-drag conversion blade and an intelligent blade. The blade form can improve the low-speed performance of the lift-type blade while keeping the high-speed performance of the blade unaltered, and it is even capable of improving the high-speed performance of the blade. With the development of microcontrol technology, this research can be widely used in existing small and medium-sized wind turbines. It is a novel type of wind energy utilization, and it will be the direction of wind turbine technology development.

Reference:

[1] GWEC. “Types of Wind Turbines (Horizontal Axis, Vertical Axis, etc.) i n context of wind turbine energy.” [Online]. Available: https://blog.truege ometry.com/tutorials/education/b633ebbda596d37cbb4a8e7cdb16d6d8/J SON_TO_ARTCL_Types_of_Wind_Turbines_Horizontal_Axis_Vertica l_Axis_etc_in_c.html. [Accessed: 04. Oct. 2025].

[2] J.A.C. Kentfiled and E.J. Claelle, “The flow physics of the Gmney flaps d evicesfor improving turbine blade performance,” *Wind Eng.*,vol. 19, no. 1, pp. 24-34, 1993. [Online]. Available: https://www.jstor.org/stable/437494 95. [Accessed: 01. Jun. 2025].

[3] N.S. Bao, F.P. Huo and Z.Q. Ye, “Aerodynamic performance influence w ith roughness on wind turbine airfoil surface,” *J. Sol. Energy*, vol. 29, no. 12, pp. 1445-1448, Dec. 2008, doi: 10.3321/j.issn:0254-0096.2005.04.00 3.

[4] W.Q. Qian and J.S. Cai, “Numerical simulation of turbulent flow past airf oil at low mach number,” *Acta Aeronaut. Astronaut. Sin.*, vol. 20, no. 3, p p. 261-264, 1999, doi: 10.3321/j.issn:1000-6893.1999.03.017.

[5] Z.F. Wang, H.J. Xia, D.Y. Li and Y.L. Feng, “Study on the influence of b lade sweep on wind turbine structure and aerodynamic characteristics,” *J. Sol. Energy*, vol. 41, no. 11, pp. 285-292, 2020, doi: 10.19912/j.0254-009 6.2020.11.039.

[6] Y.S. Liu, Z.Ye, Y.J. Han and C. Li, “Numerical Study on Aerodynamic P erformance of Wave Airfoil on Suction Side of Wind Turbine Blade,” *Th ermal power Eng.*, vol. 35, no. 07, pp. 185-191, 2020, doi: 10.16146/ j.cn ki.rndlgc.2020.07.026.

[7] J.H. Wu, C.Y. Zhu, K. Chen and T.G. Wang, “Influence of different blad e tip configurations on aerodynamic characteristics of large wind turbine blades,” *J. Eng. Thermophys.*, vol. 41, no. 11, pp. 2742-2746, Nov. 2020. [Online]. Available: https://www.cnki.net. [Accessed: 07. Oct. 2025].

[8] J. Alber, et al. “Aerodynamic effects of Gurney flaps on the rotor blades o f a research wind turbine,” *Wind Energy Sci.*, vol. 5, no. 4, pp. 1645-1662, 2020, doi: 10.5194/wes-5-1645-2020.

[9] A. Sagharichi, M.J. Maghrebi and A. ArabGolarcheh, “Variable pitch bla des:An approach for improving performance of Darrieus wind turbine,” *J. Renew. Sustain. Energy*, vol. 8, no. 5, p. 053305, 2016, doi: 10.1063/1.49 64310.

[10] Z.Z. Zhao, G.Y. Zeng, T.G. Wang, B.F. Xu and Y. Zheng, “Numerical re search on effect of transition on aerodynamic performance of wind turbin e blade with vortex generators,” *J. Renew. Sustain. Energy*, vol. 8, no. 6, p. 063308, 2016, doi:10.13334/j.0258-8013.pcsee.2016.04.018.

[11] G.Q. Li, W.G. Zhang, Y.B. Jiang and P.Y. Yang, “Experimental investiga tion of dynamic stall flow control for wind turbine airfoils using a plasma actuator,” *Energy*, vol. 185, pp. 90-101, 2019, doi: 10.1016/j.energy.2019. 07.017.

[12] F.P. Huo, H. Liu and Z.Y. Chen, “Experimental study on improving lift o f horizontal axis wind turbine blade profile,” *J. Eng. Thermophys.*, vol. 24, no. 2, pp. 220-223, Mar. 2003, doi: 10.3321/j.issn:0253-231X.2003.02.01 1.

[13] K. Jafari, M.H. Djavareshkian and B.F. Feshalami, “The Effects of Differ ent Roughness Configurations on Aerodynamic Performance of Wind Tu rbine Airfoil and Blade,” *Int. J. Renew. Energy Dev.*, vol. 6, no. 3, pp. 27 3-281, 2017, doi: 10.14710/ijred.6.3.273-281.

[14] K. Koca, M.S. Genç and H.H. Açikel, “Experimental Investigation of Sur face Roughness Effect over Wind Turbine Airfoil,” *Çukurova Üniversites i Mühendislik-Mimarlık Fakültesi Dergisi*, no. S2, pp. 127-134, 2016, doi: 10.21605/CUKUROVAUMMFD.316730.

[15] M. Zamani, M.J. Maghrebi and S.A. Moshizi, “Numericalstudy of airfoil thickness effects on the performance of J-shaped straight blade vertical ax

is wind turbine," *Wind Struct.*, vol. 22, no. 5, pp. 595-616, 2016, doi: 10.12989/was.2016.22.5.595.

[16] X.Y. Zhao, et al. "Experimental study on the characteristics of wind turbine wake field considering yaw conditions," *Energy Sci. Eng.*, vol. 9, no. 12, pp. 2333-2341, 2021, doi: 10.1002/ese3.987.

[17] R.H. Liebeck, "Design of subsonic airfoils for high lift," *J. Aircraft*, vol. 15, no. 9, pp. 547-561, 1978, doi: 10.2514/3.58406.

[18] A. Tyagi, P. Singh, A. Rao, G. Kumar and R.K. Singh, "A novel framework for optimizing gurney flaps using RBF neural network and cuckoo search algorithm," arXiv Prepr. arXiv:2307.13612, 2023, doi: arXiv:2307.13612.

[19] K. Lin, S.Q. Zhang, C.F. Liu, H.W. Yang and B. Zhang, "Aerodynamic optimization of NACA 0012 airfoils with attached Gurney flap in the rarefied gas flow," *AIP Adv.*, vol. 13, no. 12, 2023, doi: 10.1063/5.0169049.

[20] Y.Y. Jia, J.C. Zhao, W.P. Cao, Q.K. Liu and S.N. Lv, "Vortex generator effect on airfoil aerodynamic performance of the continuous Reynolds number effect analysis," *J. Hebei Univ. Sci. Technol.*, vol. 48, no. 4, pp. 464-472, 2025, doi: 10.7535/hbkd.2025yx04012.

[21] L.B. Li, et al. "Superhydrophobic bulgy windmill for synchronous efficient fog collection and power generation," *ACS Appl. Mater. Interfaces*, vol. 16, no. 12, pp. 15496-15504, 2024, doi: 10.1021/acsami.3c17709.

[22] Z.P. Qin, G.S. Wei, C. Liu and Z.D. Xiao, "Study on aerodynamic performance of wind turbine airfoil with combined S-slot and trailing edge flap control," *Power Gener. Technol.*, vol. 45, no. 1, p. 24, 2024, doi: 10.12096/j.2096-4528.pgt.22139.

[23] T.P. Syawitri, Y.Yao, J. Yao and B. Chandra, "Drag reduction of lift-type Vertical axis wind turbine with slit modified Gurney flap," *J. Wind Eng. Ind. Aerodyn.*, vol. 253, p. 105853, 2024, doi: 10.1016/j.jweia.2024.105853.

[24] A. Abdolahifar and S.M.H. Karimian, "A comprehensive three-dimensional study on Darrieus vertical axis wind turbine with slotted blade to reduce flow separation," *Energy*, vol. 248, p. 123632, 2022, doi: 10.1016/j.energy.2022.123632.

[25] H.E. Tanürün, "Aerodynamic Performance Optimization of a Vertical-Axis Wind Turbine Using Blade–Spoke Connection and Pitch Angle via the Taguchi Method," *Bull. Polish Acad. Sci. Tech. Sci.*, e156796-e156796, 2025, doi: 10.24425/bpasts.2025.156796.

[26] P. Strojny, "Study on the efficiency of small-scale wind turbine with rotor adapted for low wind speeds," *Bull. Polish Acad. Sci. Tech. Sci.*, vol. 72, no. 6, p. 151954, 2024, doi: 10.24425/bpasts.2024.151954.

[27] Y. Zhang, et al. "Investigation of aerodynamic forces and flow field of an H-type vertical axis wind turbine based on bionic airfoil," *Energy*, vol. 242, p. 122999, 2022, doi: 10.1016/j.energy.2021.122999.

[28] S.S. Ul Hassan, M.T. Javaid, U. Rauf, S. Nasir, A. Shahzad and S. Salamat, "Systematic investigation of power enhancement of Vertical Axis Wind Turbines using bio-inspired leading edge tubercles," *Energy*, vol. 270, p. 126978, 2023, doi: 10.1016/j.energy.2023.126978.

[29] H.R. Kaviani and M. Moshfeghi, "Power Generation Enhancement of Horizontal Axis Wind Turbines Using Bioinspired Airfoils: A CFD Study," *Machines*, vol. 11, no. 11, p. 998, 2023, doi: 10.3390/machines11110998.

[30] C.S. Nalavade, U.H. Rathod, U.K. Saha and V. Kulkarni, "On the Application of Bio-Inspired Sea-Pen Blades in a Savonius Wind Rotor: A Three-Dimensional Computational Analysis," *J. Energy Resour. Technol.*, vol. 1, no. 1, p. 011302, 2025, doi: 10.1115/1.4066105.